



**HAL**  
open science

# Uncertainty Quantification With Sparsely Characterized Parameters: An Example Applied to Femoral Stem Mechanics

Godlove Wanki, Stephen Ekwaro-Osire, João Paulo Dias, Americo Cunha Jr

► **To cite this version:**

Godlove Wanki, Stephen Ekwaro-Osire, João Paulo Dias, Americo Cunha Jr. Uncertainty Quantification With Sparsely Characterized Parameters: An Example Applied to Femoral Stem Mechanics. *The Journal of Verification, Validation and Uncertainty Quantification (VVUQ)*, 2020, 5 (3), pp.031005. 10.1115/1.4048749 . hal-02983497

**HAL Id: hal-02983497**

**<https://hal.science/hal-02983497>**

Submitted on 30 Oct 2020

**HAL** is a multi-disciplinary open access archive for the deposit and dissemination of scientific research documents, whether they are published or not. The documents may come from teaching and research institutions in France or abroad, or from public or private research centers.

L'archive ouverte pluridisciplinaire **HAL**, est destinée au dépôt et à la diffusion de documents scientifiques de niveau recherche, publiés ou non, émanant des établissements d'enseignement et de recherche français ou étrangers, des laboratoires publics ou privés.

Copyright

# Uncertainty Quantification With Sparsely Characterized Parameters: An Example Applied to Femoral Stem Mechanics

**Godlove Wanki**

Mem. ASME  
Department of Mechanical Engineering,  
Texas Tech University,  
Lubbock, TX 79409  
e-mail: godlove.wanki@ttu.edu

**Stephen Ekwaro-Osire**<sup>1</sup>

Fellow ASME  
Department of Mechanical Engineering,  
Texas Tech University,  
Lubbock, TX 79409  
e-mail: stephen.ekwaro-osire@ttu.edu

**João Paulo Dias**

Mem. ASME  
Department of Civil and Mechanical Engineering,  
Shippensburg University of Pennsylvania,  
Shippensburg, PA 17257  
e-mail: jpdias@ship.edu

**Americo Cunha Jr.**

Institute of Mathematics and Statistics,  
Rio de Janeiro State University,  
Rio de Janeiro, RJ 20550-900, Brazil  
e-mail: amercio.cunha@uerj.br

*The advent of state-of-the-art additive manufacturing (AM) processes has facilitated the manufacturing of complex orthopedic metallic implants such as femoral stems with porous portions based on lattice structures. These struts often have rough and not smooth textured surfaces, for which the irregularities may influence mechanical properties. To make robust predictions about the behavior of this kind of system, the variability effect of its parameters on the stem stiffness must be considered in the processes of modeling and design of porous femoral stems. Also, to improve the credibility of computational models used for hip implant analysis, which involves numerous uncertainties, there is a need for rigorous uncertainty quantification (UQ) framework for proper model assessment following a credible-modeling standard. This work proposes a UQ framework in the presence of sparsely characterized input parameters using the maximum entropy principle for analyzing a femoral stem implant model and thus to clarify how uncertainties impact the key properties of a porous femoral stem. In this study, uncertainties in the strut thickness, pore size, Young's modulus, and external forcing are considered. The UQ framework is validated using experimental results available from literature, following the guidelines set in an ASME standard. [DOI: 10.1115/1.4048749]*

*Keywords: femoral stem, uncertainty quantification, lattice structure, maximum entropy principle, kriging*

## 1 Introduction

The stiffness mismatch between femoral stems and host bone tissue fuels the need for porous femoral stems which would improve long-term clinical outcomes of total hip arthroplasty (THA). THA is one of the most performed surgical procedures, and despite the satisfactory short-term and long-term outcomes, several technical issues related to the implant design may lead to early revision surgeries [1,2]. Fully dense metallic alloys are the current standard orthopedic implants being used and studies are constantly being done to improve them due to their high stiffness when compared to bone. Probabilistic design approaches have been applied to evaluate the effect of randomness in the design parameters on the structural integrity of orthopedic implants. Dopico-González et al. [3] conducted a probabilistic investigation of an uncemented hip replacement using Monte Carlo and Latin hypercube simulations in a finite element (FE) model of a femoral stem. Easley et al. [4] developed a probabilistic FE tool to quantify the effect of uncertainty in the design variables on the performance of orthopedic components. Bah et al. [5] presented a statistical investigation into the effects of implant positioning on the initial stability of an uncemented femoral stem. Kharmanda et al. [6] used shape optimization to produce hollow stems and applied probabilistic analysis to study the boundary conditions change in a two-dimensional FE femoral stem model. Nicolella et al. [7] investigated the effect of three-dimensional prosthesis shape optimization on the probabilistic response and probability of failure of a cemented femoral stem. Other relevant probabilistic methods and analysis techniques commonly used in orthopedic biomechanics applications were reviewed in Laz and Browne [8]. The above probabilistic studies were performed on fully dense stems which frequently have mechanical complications like stress

shielding. To overcome these issues, considerable effort is being made to design more biomechanical compatible orthopedic implants made of porous materials [9] as it is well known that porous structures can reduce the stiffness of metallic femoral stems, as well as facilitate bone cell ingrowth to improve the implant fixation [10–12].

Recently, several design approaches for complex porous stems have been proposed based on topology optimization design techniques, finite element modeling, and advanced additive manufacturing (AM) technologies [11–14]. However, existing studies have pointed out that there is a higher chance of introducing uncertainties in the manufacturing of porous structures fabricated by AM processes [15]. This can result in significant uncertainties in the models used to predict the mechanical response of the porous implant, which cannot be handled by conventional deterministic design approaches [15]. Most of the current probabilistic design approaches assume probability distributions for their input random variables as there is no consensus on how to model this uncertainty in design parameters. In this context, the maximum entropy principle (MaxEnt) is a convenient method to estimate distributions because it minimizes the amount of bias that can be introduced by prior information [16].

The ASME V&V 40 framework is proposed as a method to establish the credibility of computational models [17]. This framework has been used by Morrison et al. [18] to establish the credibility of computational fluid dynamics models of a generic centrifugal pump in different contexts of use (COU). They showed that the model risk can affect the level of verification and validation activities needed to establish the credibility of the model. Parvinian et al. [19] applied the V&V 40 framework to computational population models used to test physiological closed-loop controlled systems. They remarked that to validate patient models, population differences need to be considered like the variation in using results from a healthy volunteer to validate a device to be used in a critically ill patient. To provide a credible method to evaluate the safety for medical devices, Hariharan et al.

<sup>1</sup>Corresponding author.

[20] used a computational fluid dynamics model and proposed a threshold-based validation approach; in their method, an acceptance criterion which provides the level of similarity between simulation and experimental results for a model to be considered validated was presented. Pathmanathan et al. [21] proposed a novel framework to assess the applicability of computational models for medical devices; the key emphasis of their framework was to ensure that modifications in COU are accounted for when related validation and applicability of the model is being considered.

Struts manufactured from AM processes often have rough and not smooth textured surfaces [22,23]. Furthermore, when irregularities like structural variations in strut architecture caused by the manufacturing process are implemented in FE models by using stochastic models, they are seen to match experimental results more closely. This suggests structural irregularities influence mechanical properties [23,24]. Furthermore, the variability of the mechanical properties and their impact on the stem stiffness still needs clarification. Moreover, uncertainties must be considered not only for the geometric properties (e.g., strut thickness, pore size) but also for morphological properties (e.g., porosity, surface-to-volume (SV) ratio), and material properties (Young’s modulus) [15]. Therefore, it is necessary to account for the uncertainties in FE modeling and design processes of porous femoral stems. Also, to improve the credibility of computational models used for hip implant analysis which often involves sparsely characterized parameters, there is a need for a rigorous uncertainty quantification (UQ) approach for proper model assessment through the ASME V&V 40 standard [18]. Thus, we propose in this paper a rigorous UQ framework for analyzing the femoral stem implant model to answer the research question: can the model provide an acceptable assessment on the stiffness of designed porous hip stems? This question is answered by considering the following COU: to use the model as a basic design tool to assess if the desired porous stem stiffness is being achieved, before its clinical study. In this study, the numerical testing was based on specific testing requirements extracted from ISO 7206-4 standard [25]. The proposed UQ framework was validated using experimental results available from literature which followed the guidelines set in the same test standard [11].

## 2 Methodology

**2.1 Porous Stem Model.** A CAD model of the Stryker “Secur-Fit™ MAX” 6052 0830A hip stem (Stryker Corporation, Kalamazoo, MI) was designed using Autodesk Inventor 2017 software package as shown in Fig. 1. This model was designed using limited information (dimensions in Fig. 1(a)). A portion of the stem body is made to accommodate the porous structure [12]

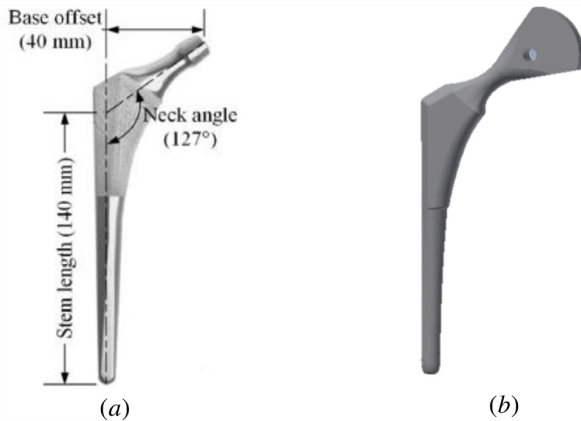


Fig. 1 Femoral stem: (a) Stryker physical model and (b) CAD model

which was a diamond cubic lattice in this study. Due to the lack of dimensions, the porous region is approximated based on the description given in Jetté et al. [12]. This 3D model is now used for FE analysis to predict the mechanical response of the femoral stem. Due to computational limitations, it is not possible to have the porous stem explicitly represented with the lattice (porous) structure in it because of the length scale difference between the implant and pores as pointed out by Simoneau et al. [11]. To alleviate this problem, the porous body is represented as a fully dense material with mechanical properties equivalent to those of the porous structure as done by Jetté et al. [12]. For the purposes of reproducibility, the femoral head used was cone-shaped similar to that in Ref. [12] as this head shape was added in their work for experimental purposes.

The FE model of the femoral stem was developed using the ANSYS Workbench 19 R1 software (ANSYS, Canonsburg, PA) to calculate the elastic response of the stem for several constant loads applied to the top of the stem. ANSYS was used without modification in this study. The setup for the FE analysis of the stem was made according to the orientations suggested in the ISO 7206-4 standard for fatigue testing of femoral stems [25] although only static testing was done in this work. The material used for the stem was Ti-6Al-4V with Young’s modulus for the fully dense and porous part of the stem of 114 GPa and 8.4 GPa, respectively. Young’s modulus of the resin was 3.7 GPa and the Poisson ratio of all the materials was assumed to be 0.3 [12]. Meshes were generated using quadratic tetrahedral elements with 28,610 elements and 49,088 nodes. For the sake of simplification, and since there is no consensus of relative movement occurring at the interface in such models [26], no friction at any interface was assumed so that both portions of the stem and the resin have fully bonded contact. The analysis was done following a similar procedure described in Jetté et al. [12] whereby a constant load was applied as a downward vertical force to the top of the femoral stem. The loads were varied linearly from 0 to 1500 N with steps of 150 N and large deflection was turned on, while the epoxy resin in which the stem had been potted was constrained to no movement in any direction. Note that the maximum force of this study was limited to 1500 N to be consistent with the force value used by Jetté et al. [12] because we intend on using those results to validate our model.

### 2.2 Uncertainty Quantification Framework

**2.2.1 Deterministic Modeling.** A schematic illustration of the deterministic modeling is shown in the flowchart on the left side of Fig. 2. The input parameters in ANSYS are material properties (Young’s modulus and Poisson ratio) and the force. For porous stem designs, Young’s modulus is dependent on the porosity of the porous region which itself is dependent on the geometric parameters strut thickness and pore size. Young’s modulus of the porous region is obtained from a power-law relationship relating, the porous region elastic modulus with porosity, and the fully dense material Young’s modulus [12]

$$E_p = E_d C (1 - \phi)^n \quad (1)$$

where  $E_p$  is the porous region Young’s modulus,  $E_d$  is the fully dense material Young’s modulus,  $\phi$  is porosity, and  $C$  and  $n$  are scaling coefficient constants. Displacement is the output obtained from ANSYS; the stiffness of the stem is calculated as the slope of the resulting force–displacement curve.

**2.2.2 Parametric Probabilistic Approach.** Robust predictions in scenarios subject to several uncertainties, such as the design of a femoral stem, demand the use of stochastic tools so that families of responses can be inferred, instead of a single nominal value. In this way, a parametric probabilistic approach is employed here to deal with the uncertainties associated with the computational model input parameters [27,28]. The parametric probabilistic approach employed in this paper involves three steps: (i)

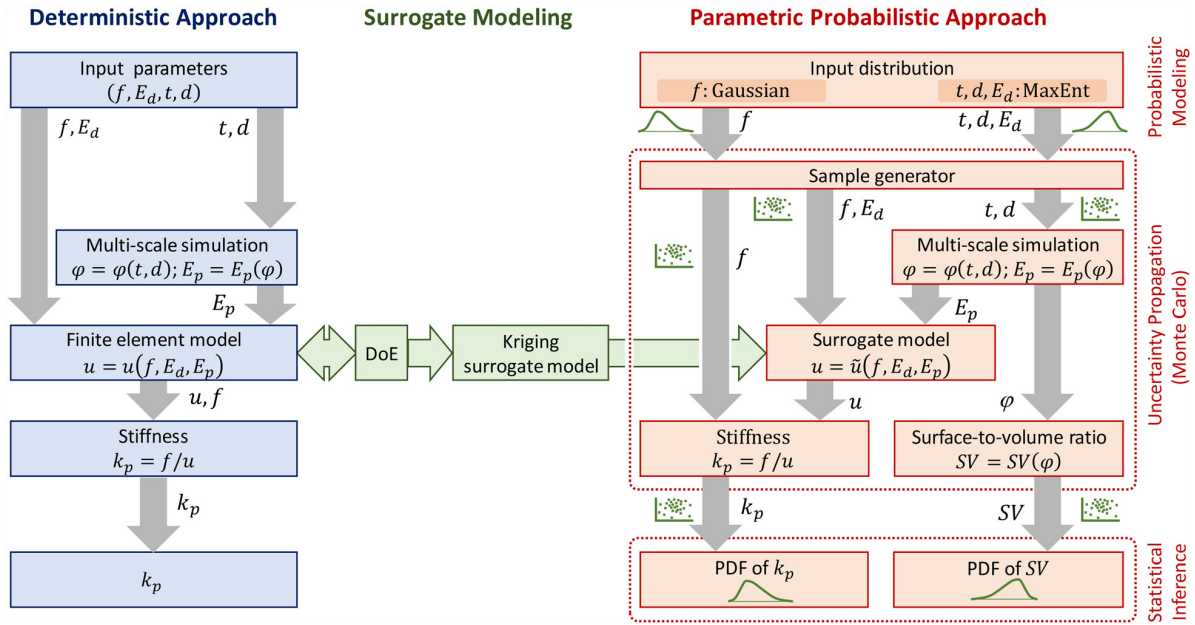


Fig. 2 Uncertainty quantification framework for porous femoral stem modeling

probabilistic modeling; (ii) propagation of uncertainties; and (iii) statistical inference. An illustration of this UQ framework is shown in Fig. 2.

**2.2.2.1 Probabilistic modeling.** In the first stage, the input parameters of the computational model subject to variability, and which consequently may affect the model's response, are identified and a probabilistic model for their joint-distribution is constructed. The following parameters are considered as random variables: (i) major pore size, (ii) strut thickness, (iii) Young's modulus of the stem's dense part, and (iv) force applied at the stem head. These four parameters are modeled by the random variables  $X_1$ ,  $X_2$ ,  $X_3$ , and  $X_4$ , respectively, for which the joint-probability distribution is specified according to the general procedure described below.

When a large set of experimental data is available, the most natural way to construct the probabilistic model (i.e., the joint-distribution) is through classical techniques of statistical inference, using nonparametric techniques (e.g., kernel density estimator) if the joint-distribution algebraic formula is not known (the most frequent case), or via parametric techniques (e.g., maximum likelihood estimator) in some special cases where an algebraic expression for the distribution is known a priori [28]. When experimental data to characterize the variability of the parameters are not available, any attempt to arbitrate a distribution and assign values to their parameters can (most likely) lead to a biased probabilistic model, capable of producing predictions that are not reliable. The consensus in the UQ field is that arbitrating probability distributions is a procedure without scientific rigor, which produces unreliable results [28,29].

On the other hand, without data, it is difficult to characterize a probability distribution. In this scenario, a very appealing technique for specifying a conservative probability distribution based on nominal information only is the MaxEnt, whose formulation incorporates all the mathematical rigor of information theory [16,28,30,31]. This inference technique deduces an algebraic formula for the joint distribution of the random variables by maximizing the entropy function associated with this distribution, respecting the restrictions imposed by the known statistical information about such sparsely characterized parameters [16,28,30,31].

Both MaxEnt and maximum likelihood are parametric statistical techniques, where an algebraic expression is used to represent

the distribution, with the parameters of this formula inferred from experimental data or theoretical information (single data). In a sense, both try to seek the best parameterization of the distribution with the available information [30,31]. The substantial difference between them is in the way the algebraic formula of the distribution is obtained. The maximum likelihood works only to identify the best parameters, the distribution formula being information provided by the user, thus being subject to possible epistemic uncertainties (an expert's judgment error, for example). Conversely, in MaxEnt, the algebraic form of the distribution is deduced from an optimization problem that has all the known information about a certain parameter as constraints. In this sense, the form of distribution is inferred from known information, thus being less subject to epistemic uncertainties. This results in the most conservative distribution in the absence of experimental data or the presence of limited experimental data [30,31].

In a scenario of probabilistic modeling with sparse information, like in this paper, it is common to see in the literature some approaches that could be considered biased, and thus less rigorous. Bias is commonly introduced by doing hypothesis about the physical and system statistical properties which are not in agreement with reality. However, it is extremely difficult (almost impossible) to construct a probabilistic model that is not biased in a sparse information setting. Literature [28,29] mathematically shows that the best approach in this case is to construct the probabilistic model that is least biased without making additional hypothesis about the statistical properties of the quantities of interest (only the known physical and statistical information must be considered). Furthermore, it is also shown that the proper mathematical tool to deal with this scenario is the information theory (used in Statistical Mechanics for several decades in much more complex systems), due to the consistency of its mathematical framework to take into account limited information about random parameters [28]. The information theory uses MaxEnt formalism to infer the least biased distribution for a quantity of interest given the known information about. This is the procedure we follow in this paper, so that the notion of rigorous employed in the paper is related to the use of a consistent mathematical tools to do the inference of the input probability distribution given a sparse information.

In the case of this paper, experimental data are not available on a large scale, so the MaxEnt-based approach is adopted to infer

the joint-distribution of the sparsely characterized parameters  $X_1$ ,  $X_2$ , and  $X_3$ . The  $X_4$  distribution is not obtained by this method since there is an available expression in the literature for this parameter and it has been used successfully in contexts with experimental validation, for which  $X_4$  is described as a constant value plus a Gaussian disturbance [32]. This procedure does not introduce bias in the modeling, because the external force does not influence the mechanical properties of the femoral stem system, thus evidencing that this random parameter is independent of the others.

In the case of the other three parameters, in principle, it is reasonable to think that they may have a certain correlation, but there are no data available to characterize this dependency. Thus, since no information of mutual correlation between these quantities is included in the list of known information, the most conservative procedure from a statistical point of view is to assume that they are all independent of each other, which is also a consequence of the MaxEnt formalism if no cross-moment information is provided.

In mathematical terms, the joint distribution of the random vector  $\mathbf{X} = (X_1, X_2, X_3)$  is obtained by maximizing the entropy function

$$H_{\mathbf{X}} = - \int_{\mathbb{R}} p_{\mathbf{X}}(x_1, x_2, x_3) \ln(p_{\mathbf{X}}(x_1, x_2, x_3)) dx_1 dx_2, dx_3 \quad (2)$$

Subject to constraints based on known statistical information

$$\int f_k(x_1, x_2, x_3) p_{\mathbf{X}}(x_1, x_2, x_3) dx_1 dx_2, dx_3 = n_k, \quad k = 0, 1, \dots, M \quad (3)$$

where  $p_{\mathbf{X}}$  is the probability density function (PDF) of the random vector  $\mathbf{X}$ , and  $f_k$  and  $n_k$ , respectively, represent known functions and values that characterize the known information (generally statistical moments) about  $\mathbf{X}$ , with  $f_0(x_1, x_2, x_3) = 1$  and  $n_0 = 1$ . This problem has an analytical solution for the most common cases of known statistical information. For further details on the MaxEnt formalism, the reader can see Refs. [16,28], and [31]. The literature provides practical limits for the values of  $X_1$  and  $X_2$ , in addition to a nominal value (mean) and a measure of dispersion (standard deviation) for each (Table 1). Whereas recognizing that experimental data is not available for sparsely characterized parameters  $X_1$ ,  $X_2$ , and  $X_3$ , their uncertainty can be modeled using the pieces of information listed in Table 1 and MaxEnt. The support and nominal value were extracted from Jetté et al. [12]. The standard deviation of  $X_1$  and  $X_2$  was estimated based on the variability expected for those parameters from manufacturing errors (given by the resolution of the additive manufacturing machine). The standard deviation of  $X_3$  was taken as 5% of the nominal value [34]. Due to physical considerations, it is also known that the marginal probability distribution of each of these parameters must fall to zero close to the support limits, as the boundary values are unlikely. On the other hand,  $X_3$  is a strictly positive parameter, with a known nominal (mean) value, whose variance is finite, as well as that of their algebraic inverse [16,28]. Taking this information into account, the MaxEnt formalism concludes that the marginal distributions of  $X_1$  and  $X_2$  are given by a nonstandard

beta distribution and  $X_3$  by a gamma distribution [28], as indicated in Table 1.

**2.2.2.2 Uncertainty propagation.** Once the probabilistic model is available, it follows a step of stochastic calculation to determine the probability distribution of the model output. This is done with the aid of the classic, but statistically robust, Monte Carlo method, where the model input uncertainties are propagated through the computational model using a sampling strategy. This technique generates samples (scenarios) independent of random parameters according to the probabilistic model constructed in Sec. 2.2.2.1 and solves the model equation for each of these, thus generating a set of output data that are postprocessed in the last stage of the framework, described in Sec. 2.2.2.3.

The samples generated for parameters the major pore size,  $d$ , and the strut thickness,  $t$ , are passed as input to the module that corresponds to the multiscale simulation where the porosity function  $\phi$  and the modulus of elasticity  $E_p$  of the porous part of the femoral stem is calculated. The porosity function  $\phi$  is used in sequence to calculate the surface-to-volume ratio (SV). On the other hand, the samples of  $E_p$ , together with scenarios generated for Young's modulus of the stem's dense part  $E_d$  and the force applied at the stem head,  $f$ , are used to calculate the displacement of the femoral stem tip  $u$ . In the sequence, the results for  $u$  generated by the surrogate model (see Sec. 2.2.3), together with the samples of force  $f$ , are used to calculate the equivalent stiffness of the femoral stem system using the formula

$$k = f/u \quad (4)$$

**2.2.2.3 Statistical inference.** The final step of this framework is a statistical inference process that uses as information the data obtained with the Monte Carlo simulation. The distribution of the following two parameters is of interest:  $k$  and SV. As explained above with regard to Young's modulus of the dense part of the stem  $E_d$ , a stiffness coefficient  $k$  is similarly well modeled by a gamma distribution, so the parameters of this probabilistic law are obtained through a parametric process of inference via the maximum likelihood estimator. In the case of SV, no algebraic form for the PDF of the distribution is known beforehand, so that the distribution of this parameter is inferred in a nonparametric way, using a kernel density estimator.

**2.2.3 Surrogate Modeling.** The natural way to compute the stem displacement would be through the FE model, but the computational cost involved in calling this module hundreds or thousands of times (e.g., Monte Carlo simulation) becomes unfeasible. In this way, a Kriging-based surrogate model is used to accelerate the calculations [35]. This approximator for the value of  $u$  is constructed with the aid of data generated within the FE module—in a procedure of design of experiments (DoE)—which are interpolated by a Gaussian stochastic process with a prescribed correlation function. More specifically, this surrogate uses an approximation of the form

$$\tilde{u} = \beta_0 + \beta_1 f + \beta_2 E_d + \beta_3 E_p + \sigma^2 Z(f, E_d, E_p) \quad (5)$$

where the central tendency (mean) of the Gaussian process is represented by  $\beta_0 + \beta_1 f + \beta_2 E_d + \beta_3 E_p$ , while  $\sigma^2 Z$  takes into

**Table 1 Sparsely characterized parameters  $d$ ,  $t$ , and  $E_d$**

Random variable	Name	Support	Nominal value	Standard deviation	MaxEnt distribution	Reference
$X_1$	Pore size	[0–1200] $\mu\text{m}$	800 $\mu\text{m}$	72.5 $\mu\text{m}^{\text{a}}$	Nonstandard beta	[12]
$X_2$	Strut thickness	[0–1000] $\mu\text{m}$	540 $\mu\text{m}$	72.5 $\mu\text{m}^{\text{a}}$	Nonstandard beta	[12]
$X_3$	Young's modulus	(0, $\infty$ ) GPa	114 GPa	5.7 GPa	Gamma	[12]

<sup>a</sup>This value is obtained as  $\frac{1}{\sqrt{12}}$  of the maximum resolution reported by the powder bed fusion additive manufacturing methods (SLS, SLM, 3DP), which is 250  $\mu\text{m}$  [33].

account statistical fluctuations, where  $\sigma^2$  is the variance and  $Z$  is the standard zero-mean unit variance Gaussian process. These parameters are identified by a statistical learning process, where the data is generated via computational experiments (design of experiments—DoE) using the FE model. Due to the excellent interpolation properties, this technique is very effective in the construction of reduced models with few samples.

**2.3 Risk-Informed Credibility Assessment.** The procedure followed to assess the credibility of the proposed model is described in the ASME V&V 40 standard [17]. This procedure was adapted from Ref. [18], and the main steps are explained in Secs. 2.3.1–2.3.4.

**2.3.1 Context of Use.** The COU defines the scope and specific role of the computational model in addressing the question of interest. In this work, the COU is associated with the use of the model as a basic design tool to assess if the desired porous stem stiffness is being achieved. It is important to mention that the model is intended to provide a preclinical assessment of the mechanical performance of the porous stem to demonstrate its initial validity for future clinical studies.

**2.3.2 Model Risk.** The evaluation of the model risk considers the possibility that the computational model leads to an incorrect decision that results in patient harm and/or other undesirable impacts. The risk assessment of the model considers the contribution of the computational model in decision-making (model influence) and the consequence of an adverse outcome resulting from an incorrect decision taken based on the model results (decision consequence). The model influence and decision consequence are determined using a three-level scale proposed in Ref. [18], and the obtained model risk based on the combined individual scores for the model influence and decision consequence is shown in a risk assessment matrix (Fig. 3).

Although the model is intended to support design assessments, the model's influence on the design sign-off decision is considered medium since the model's results will be used as a guideline for the prototyping phase, which will be ultimately be assessed with in vitro tests. On the other hand, if the model leads to an incorrect design (underestimating or overestimating the actual stem stiffness), it could result in clinical issues such as patient injury and the need for surgery revision, which makes the decision consequence of the model to be classified as high. Therefore, the overall model risk obtained from the combined scores attributed to the model influence and decision consequence is medium-high (overall risk score 4).

decision consequence	high	3	4	5
	medium	2	3	4
	low	1	2	3
		low	medium	high
		model influence		

Fig. 3 Model risk assessment matrix: model risk for COU is medium-high

**2.3.3 Selection of Credibility Factors and Goals.** The next step in the V&V process is to translate the model risk into credibility goals for several relevant credibility factors established in the ASME V&V 40 standard [17]. Among the credibility factors presented in Ref. [17], the ones relevant to this work and their respective goals are presented in Table 2, for the verification process, and Table 3, for the validation and applicability processes. For the verification process (Table 2), the main objective was to assess if the mathematical models were solved correctly by considering the software liability and calculation accuracy, and the discretization errors (DEs) caused by the computational mesh. In the validation process, the question to be addressed was if the model was able to capture the real behavior of a porous stem by comparing the model results with standard experimental test results reported in the literature. For the validation process, the most relevant credibility factors were the test conditions, assessments on the output comparisons, such as the number of outputs considered, rigor, and agreement of the comparisons. For the applicability process, the main objective was to determine the relevance of the validation activities to the context of use by determining the probabilities of having the model providing results that underestimate and overestimate the experimental results. This factor is useful to understand the applicability of the model and the risks associated with the model capability to overpredict or underpredict the test results.

**2.3.4 Verification & Validation (V&V) Plan.** Given the definitions of the question of interest, COU, model risk assessment, and credibility factors described above for the proposed problem, the next step is the definition of the V&V plan. Essentially, the execution of the V&V plan is performed in four steps:

- (1) Mesh sensitivity analysis of the FE model.
- (2) Comparison of the FE deterministic model with numerical results reported in Ref. [12] for the same stem geometry.
- (3) Statistical validation of the accuracy of the surrogate model.
- (4) Comparison between the model prediction results and experimental data reported in Ref. [12] considering uncertainties.
- (5) Assessment of the relevance of the validation results to support the applicability of the model in the COU.

Steps 1–3 of the V&V plan are used to support the verification process, whereas steps 4 and 5 are used to support the validation and applicability processes.

### 3 Results and Discussion

**3.1 Uncertainty Modeling of the Input Parameters.** Uncertainty modeling of the major pore size,  $d$ , and the strut thickness,  $t$ , of the porous stem is a challenging task through conventional parametric statistical approaches, due to the lack of experimental measurements about the variability of the geometric features of porous stems reported in the literature. Thus, as explained in section, the nonstandard beta distribution is the resulting MaxEnt distribution for  $d$  and  $t$  after solving Eq. (2) considering the known information (Table 1) and the physics of the problem. The standard deviation was calculated as  $0.29 \delta x$  according to the formulation [37], where  $\delta x$  is the resolution of the AM method used.

Figure 4 shows the PDFs of the input parameters  $d$  and  $t$ . It can be observed that the PDFs of the parameters  $d$  and  $t$  have very similar behavior and the same curve shape.

Two other model input parameters considered in this work were Young's modulus of the dense part of the stem  $E_d$  and the applied force at the stem head,  $f$ . It is important to account for uncertainties in Young's modulus because different works list different values of Young's modulus for the same material. Considering  $E_d$  as a random variable accounts for the variability found in literature; the resulting distribution of Young's modulus obtained from MaxEnt is a gamma distribution. The distribution of  $f$  is

**Table 2 Goals and credibility factors for the verification process**

Factor		Goals
Code verification	Software quality assurance (SQA)	(a) Very little or no SQA procedures were specified or followed (b) SQA procedures were specified and documented (c) In addition to the previously specified SQA procedures, the software anomaly list and the software development environment are fully understood and the impact on the COU is analyzed and documented; quality metrics are tracked
	Numerical code verification (NCV)	(a) NCV was not performed (b) The numerical solution was compared to an accurate benchmark solution from another verified code (c) The numerical solution was compared to an accurate benchmark solution, either an analytical solution or using the method of manufactured solutions (MMS) [36]
Calculation verification	Discretization error (DE)	(a) No mesh convergence analysis performed (b) Mesh convergence analysis performed; conservation equations balances not checked (c) Mesh convergence analysis performed; conservation equations balances checked; no estimation of DE (d) Mesh convergence analysis performed; conservation equations balances checked; DE estimated for problem-specific quantities of interest

**Table 3 Goals and credibility factors for the validation and applicability processes**

Factor		Goals	
Comparator	Test conditions	(a) Test conditions were qualitatively characterized (b) Few key characteristics of the test conditions were provided (c) All key characteristics of the test conditions were provided	
Assessment	Output comparison	Quantity	(a) Single output was compared (b) Multiple outputs were compared
		Rigor	(a) Only visual comparison was performed (b) Comparison performed by determining the difference between computational results and experimental results (c) Uncertainty in the output of the computational model or the comparator was used in the output comparison (d) Uncertainty in the output of the computational model and the comparator were used in the output comparison
	Agreement <sup>a</sup>	(a) Good (relative difference smaller than 5%) (b) Satisfactory (relative difference between 5% and 20%) (c) Unsatisfactory (relative difference larger than 20%)	
Applicability	Relevance of the validation activities to the COU	(a) Low probability of overestimating/underestimating the actual stiffness. Preclinical (in vitro) test for confirmation may not be needed (b) High probability of overestimating the actual stiffness/low probability of underestimating the actual stiffness. Preclinical (in vitro) test for confirmation may be needed (c) Low probability of overestimating the actual stiffness/high probability of underestimating the actual stiffness. Preclinical (in vitro) test for confirmation may be needed (d) High probability of overestimating/underestimating the actual stiffness. Preclinical (in vitro) test for confirmation may be needed	

<sup>a</sup>The goals established for this factor are selected arbitrarily for demonstration of the proposed approach only. The rigor of the validation depends on the intended use of the model predictions and the risks associated with its use.

proposed by Yosibach et al. [32] who performed a probabilistic analysis on hip forces and deduced the forces acting on a hip follow a Gaussian distribution. The force applied on the hip plays an important role in the life of femoral implants; thus, it is important to use reliable probabilistic descriptions of such forces.

Figure 5 shows the PDFs of  $E_d$  and  $f$ .

**3.2 Verification.** For the verification credibility factors shown in Table 2, the achieved selected goals are listed in Table 4. To support the numerical code verification (NCV) process, we

used the FE simulation results reported in Ref. [12] as a base for comparison with our model. The comparison between the force and vertical displacement results is shown in Fig. 6. One can observe a good agreement between our model and Jetté et al. [12] for the fully dense stem, whereas for the porous stem, our results presented a maximum absolute deviation of 16% from Jetté et al. [12]. Such deviation is credited to the lack of enough information on the dimensions of the porous part of the stem, thus based on the good agreement of the dense stem, our model can be said to solve the problem correctly.

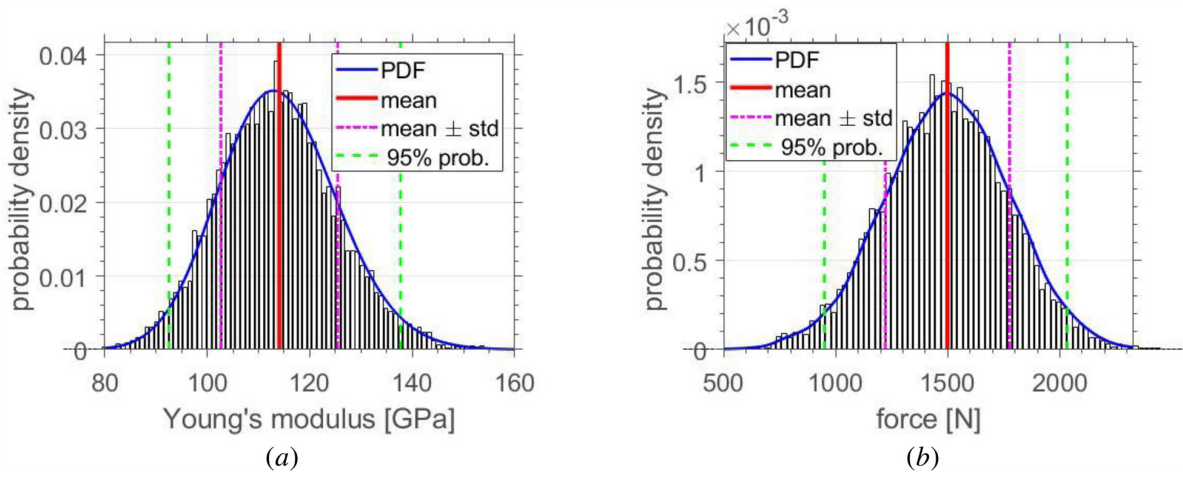


Fig. 4 MaxEnt PDFs for sparsely characterized parameters: (a) major pore size,  $d$ , and (b) strut thickness,  $t$

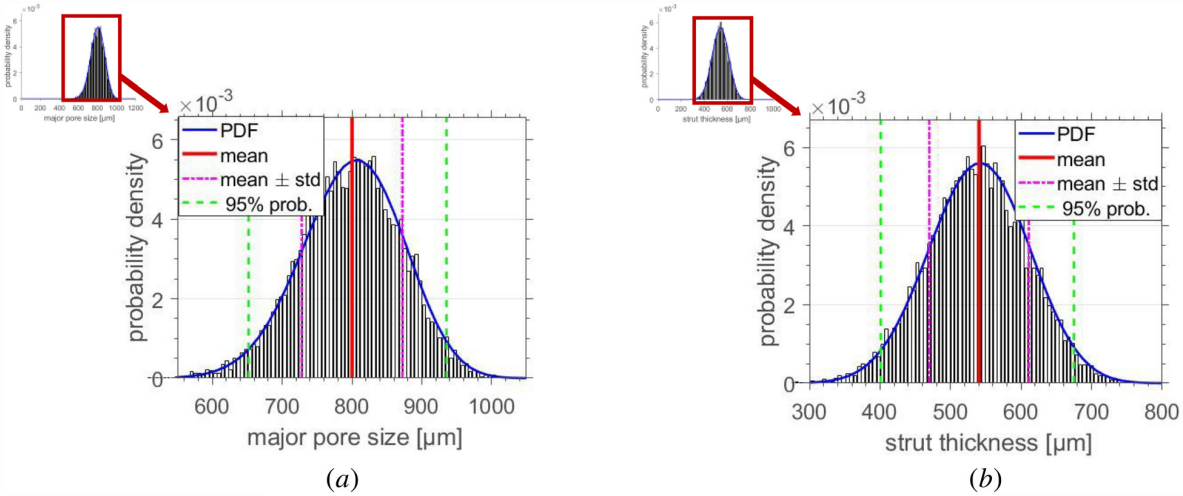


Fig. 5 PDFs for input parameters: (a) Young's modulus of the dense part of the stem,  $E_d$ , and (b) applied force at the stem head,  $f$

The calculation verification was also performed through a mesh convergence analysis of the FE model and the results are presented in Table 5. In this work, we used the fully automatic adaptive meshing convergence tool provided by ANSYS Workbench; this process provides the desired accuracy in the smallest number of runs possible. The model mesh was set to adapt to the vertical displacement of the model with a convergence criterion of 1% allowable variation in the maximum vertical displacement. After three consecutive runs, the model converged to 0.3% change in vertical displacement which we consider a satisfactory result for the mesh convergence analysis based on our predefined convergence criterion. In the second iteration, a refinement factor of 2 was used to change the element size, while in the third iteration the factor of 1.5 was used. The standard ASME V&V10.1 recommends the factor be  $> 1.3$  [40]. This mesh convergence study was performed on displacement while our quantity of interest was the stiffness. Since the analysis was within the linear range, it was assumed that the convergence of stiffness here will be similar to that of displacement.

The last step of the calculation verification process involves testing the effectiveness of the Kriging surrogate model in replacing the FE model.

Figure 7 quantitatively compares responses obtained at each training point. The small deviation of all the points from the

identity line ( $y = x$ ) demonstrates that there is a very small difference between the FE simulation and Kriging surrogate model predictions. Furthermore, the normalized empirical error of the surrogate model is  $6.4 \times 10^{-6}$ . The low error coupled with the good correlation of the FE model to surrogate model results is an indicator of the robustness of this metamodel and confirms that the Kriging surrogate model can be generalized to any prediction point within the valid range thus fully replacing the original FE model.

The numerical algorithm used to compute the MaxEnt distributions and draw the corresponding statistical samples, for a given set of known information, is implemented in *MaxEnt—Maximum Entropy Code*, an easy to run MATLAB package with robust routines and examples for MaxEnt estimation. These routines were verified by comparison with known analytical expressions in a few special, but representative, cases. The code is available at GitHub [39]. Figure 8 shows a verification test where the MaxEnt distribution for the given known information is Gamma, the estimated PDF and cumulative density function (CDF) are both presented and compared with their counterparts computed with MATLAB routines. It can be seen that the PDF and CDF estimations are robust.

**3.3 Validation and Applicability.** The validation and applicability credibility factors for the achieved selected goals are also

**Table 4 Selected goals for the applied credibility factors**

Activities		Credibility factor	Selected goal	Justification
Verification	Code	Software quality assurance (SQA)	(a)	A rigorous code verification was not performed since it was out of scope. For the SQA, the code tests performed by the vendor [38] were used. For rigorous code verification procedures in commercial code, see Ref. [36]
		Numerical code verification (NCV)	(b)	A code-to-code comparison test was performed by comparing the porous stem stiffness (quantity of interest) calculated with the proposed FE model with the numerical solution presented by Jetté et al. [12] for the same problem. For the surrogate model, the results for the quantity of interest were compared with the original FE model results. The numerical algorithm used to compute the MaxEnt distributions and the corresponding statistical samples was verified with benchmark tests where the MaxEnt distribution for the given information is known [39].
	Calculation	Discretization error (DE)	(b)	In the FE model, a simple grid convergence analysis was carried out in the porous stem geometry to determine if the quantity of interest is sensitive to the mesh parameters. For the surrogate model, the calculation error was estimated by calculating the percentage deviation from the original FE model. Calibration validation. Test statistical validation. Cost function results
Validation	Comparator	Test conditions	(c)	The experimental tests were run by Jetté et al. [12] following the ISO 7206-4 standard. Results for the porous stem stiffness calculated from the force and displacement diagram followed by their respective uncertainties were provided
	Assessment (Output comparison)	Quantity	(a)	Since the COU of the present model covers only the stiffness of the porous stem as the quantity of interest, comparisons were drawn only for this quantity
		Rigor	(d)	A comparison considering uncertainties in both experimental data and model results was carried out to provide sufficient evidence of the model's credibility. Throughout uncertainty quantification of the model is deemed necessary for the COU to provide more reliable design assessment and reduce the number of standard physical tests to evaluate the actual stiffness of porous stems
		Agreement	(b)	The calculated relative difference between the experimental and numerical mean porous stiffness was around 11%. This agreement is considered satisfactory for this study.
Applicability		Relevance of the validation activities to the COU	(c)	The model has a probability to overestimate the actual stiffness below 3%, whereas the probability to underestimate the actual stiffness was above 95%. However, preclinical (in vitro) tests may be needed to confirm the model predictions.

**Table 5 Results for mesh convergence analysis of the FE model**

	# of nodes	# of elements	Maximum vertical displacement (mm)	Change in the maximum vertical displacement (%) <sup>a</sup>
1	16,468	9025	1.059	—
2	33,586	18,409	1.136	7.0
3	49,088	28,610	1.133	0.3

<sup>a</sup>Change =  $|\frac{u_{n+1} - u_n}{u_n}| \times 100$ ; where  $n = 1, 2, 3$ .

listed in Table 4. The experimental tests were carried out by Jetté et al. [12], in which they followed an ISO 7206-4 standard test procedure described in Ref. [25]. For the output comparison factors, the rigor of the comparison between the numerical and experimental with uncertainties results, and the level of agreement between them are supported by the results shown in Fig. 9. This figure shows the mean values for the experimental and numerical stiffness and their respective 95% probability confidence interval. For the numerically calculated stiffness, the confidence interval

was obtained from the distributions shown in Fig. 10. For the experimental stiffness, the confidence interval was taken from the variability of the experimental data provided in Ref. [12]. By comparing the experimental and numerical mean stiffness values only, one can see that the relative difference between them was about 11%, which was considered satisfactory (see the selected goal for the output comparison agreement in Table 4). It is important to mention that this criterion was arbitrarily selected for demonstration purposes of the proposed framework only, and that

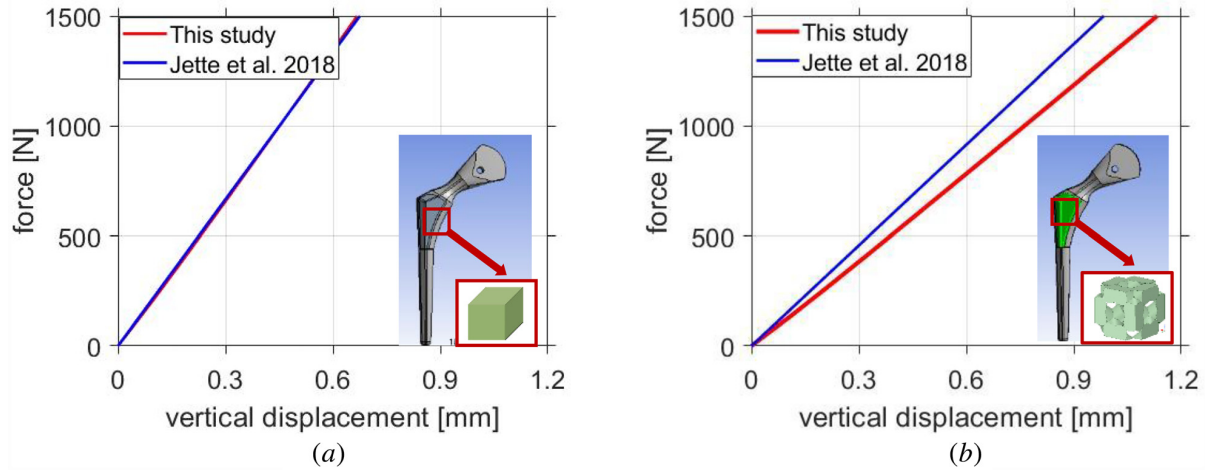


Fig. 6 Force–displacement plots of (a) the fully dense and (b) porous stem

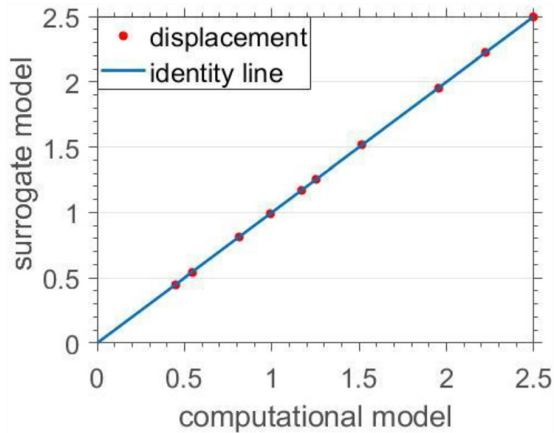


Fig. 7 Calculation verification of the surrogate model

rigor of the framework validation depends on the intended use of the model predictions and the risks associated with its use. Moreover, it can be seen from the graph that all the experimental results for the stiffness of the porous stem fall within the numerically predicted 95% confidence interval. Thus, the UQ framework can be considered validated to predict the stiffness of the porous stem, once the numerical prediction encompasses, very likely, the experimental results. In addition to the comparison of the numerical and experimental results shown in Fig. 9, it also includes 2 prediction points. Prediction point 1, is for a mean pore size of  $500\ \mu\text{m}$  and point 2 was with a mean pore size of  $300\ \mu\text{m}$ . The model predicted stiffness values of  $1291 \pm 176\ \text{N/mm}$  and  $1327 \pm 191\ \text{N/mm}$ , respectively, for both prediction points. Based on the rigor of the proposed UQ framework, the model can be considered credible enough to predict the stiffness values of a porous femoral stem as it can be seen that for both prediction points, the predicted stiffness 95% confidence interval produces acceptable results for the stiffness of porous stems [12].

Furthermore, considering the limits of the confidence interval for the experimental results and the probability distribution calculated for the porous stem stiffness (see Fig. 10), an assessment on the model applicability the COU was provided based on the goals established in Table 3. According to the validation results, it was found that the probabilities of the model overestimate and underestimate the stiffness of the actual porous stem are 2.6% and 95.4%, respectively (see Table 4). Since the probability of

underestimation is too high compared to the probability of overestimation, the model applicability in the COU may require preclinical in vitro tests to confirm the model predictions. Finally, the predictability of the uncertainty level in the stiffness of the porous stem is relevant from a design perspective because it allows the designer to address more reliable design solutions. Depending on the design requirements, the statistical parameters of the model input random variables (e.g., mean and standard deviation) can be tailored to minimize the risk of the model to overestimate or underestimate the actual behavior of the porous stem and provide a more confident design assessment compared to a deterministic design approach.

**3.4 Probability Distributions of Output Parameters.** In our probabilistic analysis, uncertainties in numerical model inputs were propagated into model equations (Eq. (5)) resulting in probability distributions of the numerically computed outputs. The validation of our model means the output values can be considered generally accepted. These input random variables have been considered in prior studies and shown to have a role in influencing the risk of failure of implants [12,41]; other studies have shown that the output, femoral stem stiffness plays an important role in bone remodeling and stress shielding [42,43]. The output SV of the porous stem is an important parameter that affects implant fixation. Our study shows that the variability of input parameters had a noticeable effect on the output as introducing variation in  $d$  and  $t$  resulted in a stiffness distribution with a mean value of  $1263\ \text{N/mm}$  compared to a nominal value of  $1316.8\ \text{N/mm}$  which was the result of the deterministic case. So, it is not sufficient to use a single value for input variables like is done in deterministic analysis, but rather a rigorous UQ approach might be needed.

**3.4.1 Porosity.** In the design of porous implants, the porosity features are very important and the FDA [44] specified a range of 30–70% for porous structures which are to permit fixation via bone ingrowth. Porosity is defined as the ratio of the volume of voids to the total volume of the entire porous region. For this work, an equation (see Appendix) representing porosity was approximated from the curve relating  $d$ ,  $t$ , and  $\phi$  presented in the Jetté et al. study [12]. Propagating the uncertainties from  $d$  and  $t$  into the porosity equation results in the PDF of porosity shown in Fig. 11(a). The distribution of the porosity is obtained using the kernel density estimator since there is no known algebraic PDF for the distribution of porosity. The limits of porosity for our study are consistent with the FDA recommended range.

The distribution of the porous Young’s modulus is obtained after propagating uncertainties from porosity,  $\phi$ , into porous

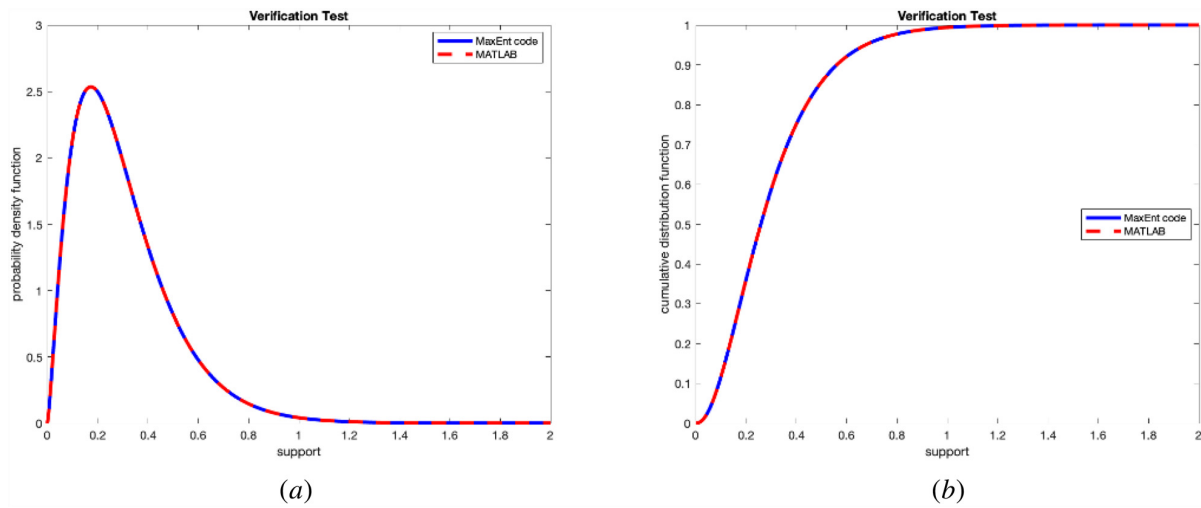


Fig. 8 Verification of MaxEnt code: (a) PDF and (b) CDF [39]

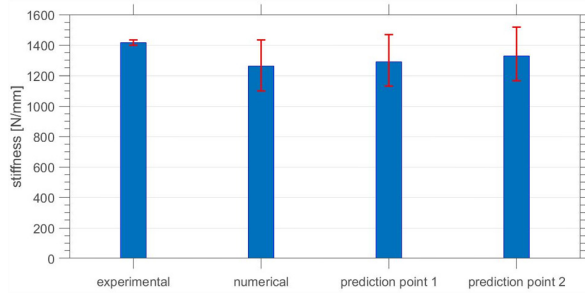


Fig. 9 Stiffness results for the femoral stem to assess the validation process

young's modulus equation (Eq. (1)). Since it is known that the distributions of material properties like Young's modulus follow a gamma distribution [28], the  $E_p$  samples are fitted using the maximum likelihood method. The gamma distribution fit looks accurate, thus giving us confidence in the  $E_p$  values obtained after the

uncertainty propagation process. This distribution is shown in Fig. 11(b).

3.4.2 *Displacement.* The model equation of the displacement was obtained from the surrogate model and the resulting PDF of displacement is calculated from the propagation of uncertainties in the force, Young's modulus of dense regions, and Young's modulus of the porous region for the porous stem into Eq. (5). The distribution of displacement is shown in Fig. 12.

3.4.3 *Stiffness.* Stiffness is a very important parameter for femoral stems and since femoral stems replace bone, it would be ideal if their stiffness value is close to that of bone. In this study, the stiffness is calculated in the presence of input parameter uncertainties. Figure 10 shows the PDFs of stiffness for the porous stem with a range of stiffness values of 1099–1432 N/mm for 95% confidence interval for the stem. The distribution of the stiffness follows a gamma distribution as is expected [28]. From the analysis of the force–displacement diagrams of Fig. 6, the stiffness obtained deterministically was 1316.8 N/mm. This value is within the 95% confidence interval range for the stiffness probability distribution with a probability associated with obtaining it. The distribution gives us the information we otherwise cannot have if the

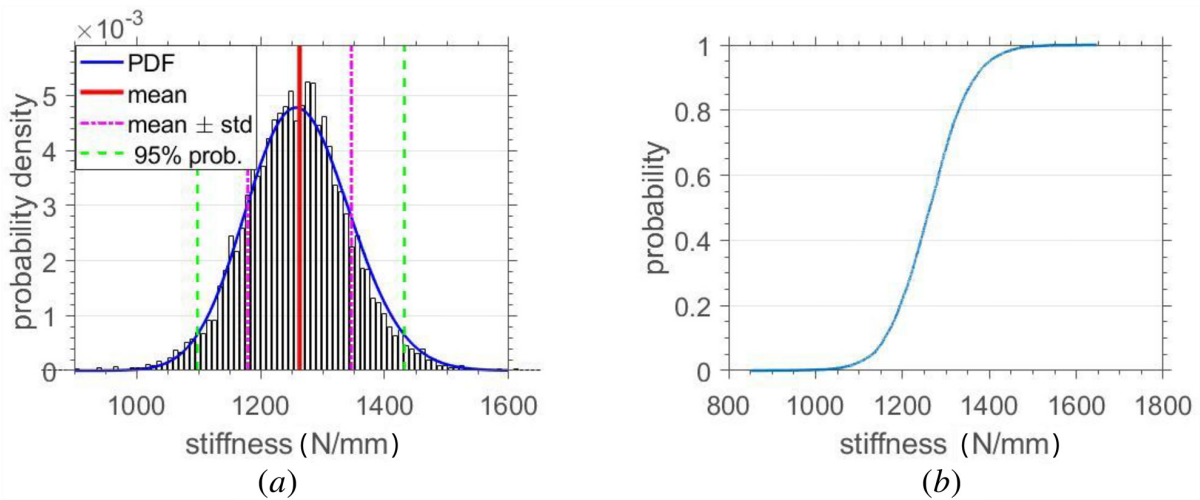


Fig. 10 Probability distribution for porous stem stiffness,  $k$ : (a) PDF and (b) CDF

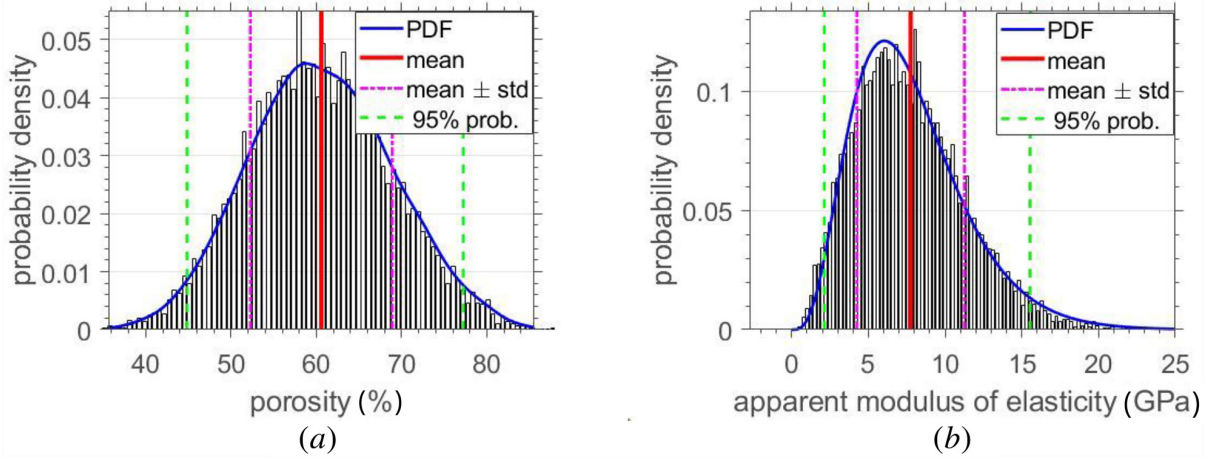


Fig. 11 PDF for (a) porosity,  $\phi$ , and (b) porous Young's modulus,  $E_p$

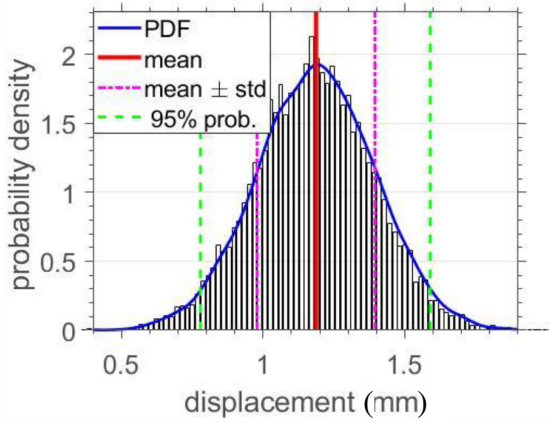


Fig. 12 PDF for displacement

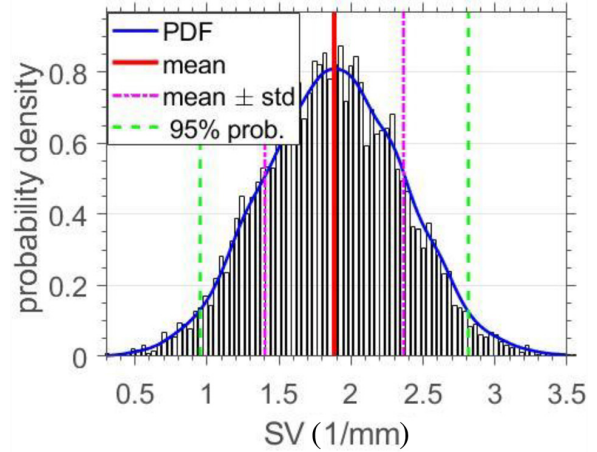


Fig. 13 PDF for surface-to-volume ratio, SV

stiffness is determined only from a deterministic point of view. Additionally, with the CDF of stiffness (Fig. 10(b)), we can determine the probability of obtaining desired values of  $k$  and as a result, evaluate the effects considering uncertainties can have on stem stiffness. For example, considering the result obtained from the deterministic analysis for,  $k$  (1316.8 N/mm), Fig. 10(b) shows that the probability of obtaining a porous femoral stem stiffness of 1316.8 N/mm and above is about 25% which means getting a stiffness of 1316.8 N/mm is not certain as deterministic studies put it. But rather there is a probability of obtaining such a value of stiffness.

**3.4.4 Surface-to-Volume Ratio.** Studies have found that porous implants provide a firm bone fixation if the SV of the porous structure approaches that of bone, which is in the range of 3–5  $\text{mm}^{-1}$  [45,46]. This makes the SV an important property to evaluate when dealing with porous structures. The SV depends on the modeling input parameters pore size and struts thickness, and, therefore, porosity. The PDF of the SV of the stem porous region can be seen in Fig. 13. For this particular study, i.e., considering  $d = 800 \mu\text{m}$  and  $t = 540 \mu\text{m}$  the 95% confidence interval for SV is 0.95–2.82  $\text{mm}^{-1}$  with a mean value of 1.88  $\text{mm}^{-1}$ . The importance of SV in determining how a porous construct will perform as an implant for bone fixation makes it important to consider uncertainties when calculating this value. The SV value in the

scenario considered in this study is low in comparison with that of bone but this property is highly dependent on  $d$  and thus a different value of  $d$  can result in more acceptable values of SV [12].

#### 4 Contribution and Future Studies

The contribution of this study is the proposed framework for uncertainty quantification in the presence of sparsely characterized parameters using the MaxEnt principle and the integration of this approach with recent developments in the V&V methodology. The MaxEnt formalism, which is based on the information theory, provides an optimal and least-biased approach to specify a consistent probability distribution in a scenario where only a sparse set of information is available. The proposed UQ framework was validated using experimental results available from literature which followed the guidelines set in the ISO 7206-4 standard [25]. In this paper, rigorous code verification was not performed since it out of the scope. For future studies, a rigorous verification is recommended, using, for example, the method of manufactured solutions (MMS) that has successfully been applied to commercial finite element code for elastostatic solid mechanics analyses [36]. Although numerical error estimation was out of the scope of this paper, it is recommended the future studies involving rigorous mesh refinement using Richardson extrapolation and calculations of a grid convergence index should be performed [47].

## 5 Conclusions

This study presented a UQ framework to assess the stiffness and surface-to-volume-ratio of a porous femoral stem model, which is part of a total hip implant. The objective was to account for uncertainties in the input parameters and see how this affects the femoral stem stiffness and surface-to-volume ratio. The probabilistic modeling involved predicting input distribution by use of the MaxEnt principle which is used in cases with limited information like in this study. A Kriging surrogate model for the ANSYS FE model output displacement was developed using information obtained from ANSYS DoE. Uncertainties from the input parameters were then propagated into the surrogate model to determine displacement and eventually stem stiffness. The model and UQ framework used for the analysis were verified and validated and further used to demonstrate how PDFs and CDFs can be used by designers to design implants that satisfy given conditions. Furthermore, the results demonstrated that uncertainties do affect porous femoral stem output properties like stiffness.

The rigorous UQ framework used to quantify uncertainties in the porous femoral stem input parameters is based on the limited information we could find about these parameters in literature. The MaxEnt was considered as a viable method to provide the probability distributions for the input parameters. The limitation of the MaxEnt is that the accuracy of the probability distribution estimated with the MaxEnt is sensitive to the quality of the information available. If poor quality information is available, or if poor quality experiments were carried out, it may compromise the quality of the information and lead to poor estimations of the uncertainties of a random variable using MaxEnt. Although the UQ framework has been shown to work for femoral stems, there is a need for probabilistic analysis which is performed on a FE system made of an implant/bone construct under realistic biomechanical loading. In the more realistic FE model (implant/bone model), the UQ framework and probabilistic methods could be extended to examine how uncertainties in stem design can affect other performance metrics like implant micromotion, wear, and other metrics of interest. The results of this study show that the UQ framework can deliver more robust design alternatives in a single analysis which represents an improvement over prior deterministic design analysis.

## Nomenclature

AM	= additive manufacturing
$C$	= scaling coefficient constant
CDF	= cumulative density function
COU	= context of use
$d$	= major pore size, $\mu\text{m}$
DoE	= design of experiments
$E_d$	= Young's modulus of dense portion of the stem, GPa
$E_p$	= Young's modulus of porous portion of the stem, GPa
$f$	= force, N
FDA	= U.S. Food and Drug Administration
FE	= finite element
$H_X$	= maximizing the entropy function
$k$	= stiffness, N/mm
MaxEnt	= maximum entropy principle
$n$	= scaling coefficient constant
PDF	= probability density function
SV	= surface-to-volume ratio, $\text{mm}^{-1}$
$t$	= strut thickness, $\mu\text{m}$
THA	= total hip arthroplasty
$u$	= displacement, mm
UQ	= uncertainty quantification
V&V	= verification and validation
$Z$	= standard zero-mean unit
$\delta x$	= additive manufacturing process resolution
$\sigma^2$	= variance
$\varphi$	= porosity, %

## Appendix

This appendix gives complementary information on the regression curve fitting parameters used to get the porosity and surface-to-volume ratio of the porous stem. The equation for porosity is a second-order polynomial of  $d$  obtained from nonlinear regression analysis of data in the literature and the equation is given below as:

$$\varphi = Ad^2 + Bd + C$$

where  $\varphi$  is porosity,  $d$  is pore size, and  $A$ ,  $B$ , and  $C$  are regression coefficients.  $A$  and  $B$  were fitted with an exponential fit as a function of  $t$ , and  $C$  had a sinusoidal fit as an of a function of  $t$

$$A = A_0e^{A_1t} + A_2e^{A_3t}$$

$$B = B_0e^{B_1t} + B_2e^{B_3t}$$

$A_0, \dots, A_3$  and  $B_0, \dots, B_3$  are constant coefficients and  $t$  is strut thickness

$$C = C_0 \sin C_1t + C_2 + C_3 \sin C_4t + C_5$$

where  $C_0, \dots, C_5$  are constant coefficients and  $t$  is strut thickness (Tables 6 and 7)

**Table 6** Coefficients of the fitted equation for porosity,  $\varphi$

$n$	$A_n$	$B_n$	$C_n$
0	-0.002765	1.028	5.329
1	-0.01442	-0.01195	0.00575
2	-0.00004219	0.1668	0.01958
3	-0.0009564	-0.001048	-0.9111
4	n/a	n/a	0.0143
5	n/a	n/a	4.413

**Table 7** Coefficients of the fitted equation for the stiffness-to-volume ratio, SV

$P_n$	$a_n$	$b_n$
0	-0.0033	-3.2124
1	0.0162	31.9020
2	-0.0826	-43.8670
3	0.0846	61.2880
4	-0.0204	-40.992

To propagate uncertainty from porosity,  $\varphi$ , to the surface-to-volume ratio, SV, a fourth-order polynomial equation was fitted using a nonlinear regression method from data available in the literature [12]

$$Y = \sum_{n=0}^4 P_n \varphi^n$$

where  $Y$  corresponds to SV,  $\varphi$  is porosity, and  $P_0, \dots, P_4$  are regression coefficients, which were fitted as linear functions of the major pore size,  $l$ , as

$$P_n = a_n l + b_n$$

in which  $a_n$  and  $b_n$  are the linear coefficients, and their values can be found above.

## References

- [1] Learmonth, I. D., Young, C., and Rorabeck, C., 2007, "The Operation of the Century: Total Hip Replacement," *Lancet*, **370**(9597), pp. 1508–1519.

- [2] Pivec, R., Johnson, A. J., Mears, S. C., and Mont, M. A., 2012, "Hip Arthroplasty," *Lancet*, **380**(9855), pp. 1768–1777.
- [3] Dopico-González, C., New, A. M., and Browne, M., 2009, "Probabilistic Analysis of an Uncemented Total Hip Replacement," *Med. Eng. Phys.*, **31**(4), pp. 470–476.
- [4] Easley, S. K., Pal, S., Tomaszewski, P. R., Petrella, A. J., Rullkoetter, P. J., and Laz, P. J., 2007, "Finite Element-Based Probabilistic Analysis Tool for Orthopaedic Applications," *Comput. Methods Programs Biomed.*, **85**(1), pp. 32–40.
- [5] Bah, M. T., Nair, P. B., Taylor, M., and Browne, M., 2011, "Efficient Computational Method for Assessing the Effects of Implant Positioning in Cementless Total Hip Replacements," *J. Biomech.*, **44**(7), pp. 1417–1422.
- [6] Kharmanda, G., Shokry, A., Antypas, I., and El-Hami, A., 2018, "Probabilistic Analysis for Osseointegration Process of Hollow Stem Used in Un-Cemented Hip Prosthesis," *J. Uncertainties Reliab. Multiphysical. Syst.*, **2**(2), pp. 1–15.
- [7] Nicoletta, D. P., Thacker, B. H., Katoozian, H., and Davy, D. T., 2006, "The Effect of Three-Dimensional Shape Optimization on the Probabilistic Response of a Cemented Femoral Hip Prosthesis," *J. Biomech.*, **39**(7), pp. 1265–1278.
- [8] Laz, P. J., and Browne, M., 2010, "A Review of Probabilistic Analysis in Orthopaedic Biomechanics," *Proc. Inst. Mech. Eng., Part H*, **224**(8), pp. 927–943.
- [9] Murr, L. E., 2017, "Open-Cellular Metal Implant Design and Fabrication for Biomechanical Compatibility With Bone Using Electron Beam Melting," *J. Mech. Behav. Biomed. Mater.*, **76**, pp. 164–177.
- [10] Arabnejad, S., Johnston, R. B., Pura, J. A., Singh, B., Tanzer, M., and Pasini, D., 2016, "High-Strength Porous Biomaterials for Bone Replacement: A Strategy to Assess the Interplay Between Cell Morphology, Mechanical Properties, Bone Ingrowth and Manufacturing Constraints," *Acta Biomater.*, **30**, pp. 345–356.
- [11] Simoneau, C., Terriault, P., Jetté, B., Dumas, M., and Brailovski, V., 2017, "Development of a Porous Metallic Femoral Stem: Design, Manufacturing, Simulation and Mechanical Testing," *Mater. Des.*, **114**, pp. 546–556.
- [12] Jetté, B., Brailovski, V., Dumas, M., Simoneau, C., and Terriault, P., 2018, "Femoral Stem Incorporating a Diamond Cubic Lattice Structure: Design, Manufacture and Testing," *J. Mech. Behav. Biomed. Mater.*, **77**, pp. 58–72.
- [13] Park, J., Sutradhar, A., Shah, J. J., and Paulino, G. H., 2018, "Design of Complex Bone Internal Structure Using Topology Optimization With Perimeter Control," *Comput. Biol. Med.*, **94**, pp. 74–84.
- [14] Al-Tamimi, A. A., Fernandes, P. R. A., Peach, C., Cooper, G., Diver, C., and Bartolo, P. J., 2017, "Metallic Bone Fixation Implants: A Novel Design Approach for Reducing the Stress Shielding Phenomenon," *Virtual Phys. Prototyping*, **12**(2), pp. 141–151.
- [15] Gorgulurslan, R. M., Choi, S.-K., and Saldana, C. J., 2017, "Uncertainty Quantification and Validation of 3D Lattice Scaffolds for Computer-Aided Biomedical Applications," *J. Mech. Behav. Biomed. Mater.*, **71**, pp. 428–440.
- [16] Cunha, A., 2017, "Modeling and Quantification of Physical Systems Uncertainties in a Probabilistic Framework," *Probabilistic Prognostics and Health Management of Energy Systems*, S. Ekworo-Osire, A. Gonçalves, and F. M. Alemayehu, eds., Springer, Cham, Switzerland, pp. 127–156.
- [17] ASME Standard, 2018, *Assessing Credibility of Computational Modeling Through Verification and Validation: Application to Medical Devices*, Vol. 40, ASME V&V, New York, Standard No. ASME V&V 40–2018.
- [18] Morrison, T. M., Hariharan, P., Funkhouser, C. M., Afshari, P., Goodin, M., and Horner, M., 2019, "Assessing Computational Model Credibility Using a Risk-Based Framework: Application to Hemolysis in Centrifugal Blood Pumps," *ASAIO J.*, **65**(4), pp. 349–360.
- [19] Parvinian, B., Pathmanathan, P., Daluwatte, C., Yaghoubi, F., Gray, R. A., Weininger, S., Morrison, T. M., and Scully, C. G., 2019, "Credibility Evidence for Computational Patient Models Used in the Development of Physiological Closed-Loop Controlled Devices for Critical Care Medicine," *Front. Physiol.*, **10**, p. 220.
- [20] Hariharan, P., D'Souza, G. A., Horner, M., Morrison, T. M., Malinauskas, R. A., and Myers, M. R., 2017, "Use of the FDA Nozzle Model to Illustrate Validation Techniques in Computational Fluid Dynamics (CFD) Simulations," *PLoS One*, **12**(6), p. e0178749.
- [21] Pathmanathan, P., Cordeiro, J. M., and Gray, R. A., 2019, "Comprehensive Uncertainty Quantification and Sensitivity Analysis for Cardiac Action Potential Models," *Front. Physiol.*, **10**, p. 721.
- [22] Harrysson, O. L. A., Cansizoglu, O., Marcellin-Little, D. J., Cormier, D. R., and West, H. A., 2008, "Direct Metal Fabrication of Titanium Implants With Tailored Materials and Mechanical Properties Using Electron Beam Melting Technology," *Mater. Sci. Eng. C*, **28**(3), pp. 366–373.
- [23] Egan, P. F., 2019, "Integrated Design Approaches for 3D Printed Tissue Scaffolds: Review and Outlook," *Materials*, **12**(15), p. 2355.
- [24] Campoli, G., Borleffs, M. S., Amin Yavari, S., Wauthle, R., Weinans, H., and Zadpoor, A. A., 2013, "Mechanical Properties of Open-Cell Metallic Biomaterials Manufactured Using Additive Manufacturing," *Mater. Des.*, **49**, pp. 957–965.
- [25] International Organization for Standardization, 2010, "Implants for Surgery—Partial and Total Hip Joint Prostheses—Part 4: Determination of Endurance Properties and Performance of Stemmed Femoral Components," ISO, Geneva, Switzerland, Standard No. ISO 7206–4.
- [26] Taylor, M., and Prendergast, P. J., 2015, "Four Decades of Finite Element Analysis of Orthopaedic Devices: Where Are We Now and What Are the Opportunities?," *J. Biomech.*, **48**(5), pp. 767–778.
- [27] Soize, C., 2013, "Stochastic Modeling of Uncertainties in Computational Structural Dynamics—Recent Theoretical Advances," *J. Sound Vib.*, **332**(10), pp. 2379–2395.
- [28] Soize, C., 2017, *Uncertainty Quantification: An Accelerated Course With Advanced Applications in Computational Engineering*, Springer, Cham, Switzerland.
- [29] Oden, J. T., 2017, "Foundations of Predictive Computational Science," The University of Texas at Austin, Austin, TX, ICES Report No. 17–01.
- [30] Shannon, C. E., 1948, "A Mathematical Theory of Communication," *Bell Syst. Tech. J.*, **27**(3), pp. 379–423.
- [31] Kapur, J. N., and Kesavan, H. K., 1992, "Entropy Optimization Principles and Their Applications," *Entropy and Energy Dissipation in Water Resources*, V. P. Singh, and M. Fiorentino, eds., Springer, Dordrecht, The Netherlands, pp. 3–20.
- [32] Yosibash, Z., Wille, H., and Rank, E., 2015, "Stochastic Description of the Peak Hip Contact Force During Walking Free and Going Upstairs," *J. Biomech.*, **48**(6), pp. 1015–1022.
- [33] Ngo, T. D., Kashani, A., Imbalzano, G., Nguyen, K. T. Q., and Hui, D., 2018, "Additive Manufacturing (3D Printing): A Review of Materials, Methods, Applications and Challenges," *Compos. Part B*, **143**, pp. 172–196.
- [34] Gibson, L. J., Ashby, M. F., and Harley, B. A., 2010, *Cellular Materials in Nature and Medicine*, Cambridge University Press, Cambridge, UK.
- [35] Slot, R. M. M., Sørensen, J. D., Sudret, B., Svenningsen, L., and Thøgersen, M. L., 2020, "Surrogate Model Uncertainty in Wind Turbine Reliability Assessment," *Renewable Energy*, **151**, pp. 1150–1162.
- [36] Aycock, K. I., Rebelo, N., and Craven, B. A., 2020, "Method of Manufactured Solutions Code Verification of Elastostatic Solid Mechanics Problems in a Commercial Finite Element Solver," *Comput. Struct.*, **229**, p. 106175.
- [37] ISO, 2008, "Evaluation of Measurement Data—Guide to the Expression of Uncertainty in Measurement," International Organization for Standardization, Paris, France, Standard No. ISO/IEC Guide 98–3.
- [38] ANSYS, 2019, "ANSYS Workbench Verification Manual," ANSYS, Canonsburg, PA.
- [39] Cunha, Jr., A., "MaxEnt—Maximum Entropy Code," GitHub, GitHub Repository, accessed Sept. 13, 2020, <https://americocunhajr.github.io/MaxEnt>
- [40] ASME, 2012, "An Illustration of the Concepts of Verification and Validation in Computational Solid Mechanics," ASME, New York, Standard No. ASME V&V 10.1.
- [41] Gillies, R. M., Morberg, P. H., Bruce, W. J. M., Turnbull, A., and Walsh, W. R., 2002, "The Influence of Design Parameters on Cortical Strain Distribution of a Cementless Titanium Femoral Stem," *Med. Eng. Phys.*, **24**(2), pp. 109–114.
- [42] Frost, H. M., 1994, "Wolff Law and Bones Structural Adaptations to Mechanical Usage—An Overview for Clinician," *Angle Orthodontist*, **64**(3), pp. 175–188.
- [43] Huiskes, R., Weinans, H., and Rietbergen, B. Van, 1992, "The Relationship Between Stress Shielding and Bone Resorption Around Total Hip Stems and the Effects of Flexible Materials," *Clin. Orthop. Relat. Res.*, (274), pp. 124–134.
- [44] FDA, 2016, "Hip Joint Metal/Polymer/Metal Semi-Constrained Porous-Coated Uncemented Prosthesis," Food and Drug Administration, Department of Health and Human Services, Medical devices, Silver Spring, MD, Standard No. 21CFR888.3358.
- [45] Martin, B., 1984, "Porosity and Specific Surface of Bone," *Crit. Rev. Biomed. Eng.*, **10**(3), pp. 179–222.
- [46] Coelho, P. G., Fernandes, P. R., Rodrigues, H. C., Cardoso, J. B., and Guedes, J. M., 2009, "Numerical Modeling of Bone Tissue Adaptation—A Hierarchical Approach for Bone Apparent Density and Trabecular Structure," *J. Biomech.*, **42**(7), pp. 830–837.
- [47] Oberkampf, W. L., and Roy, C. J., 2010, *Verification and Validation in Scientific Computing*, Cambridge University Press, London.